

Valence Force Model for Phonons in Graphene and Carbon Nanotubes

Vasili Perebeinos* and J. Tersoff†

IBM Research Division, T. J. Watson Research Center, Yorktown Heights, New York 10598

(Dated: August 25, 2021)

Many calculations require a simple classical model for the interactions between sp^2 -bonded carbon atoms, as in graphene or carbon nanotubes. Here we present a new valence force model to describe these interactions. The calculated phonon spectrum of graphene and the nanotube breathing-mode energy agree well with experimental measurements and with *ab initio* calculations. The model does not assume an underlying lattice, so it can also be directly applied to distorted structures. The characteristics and limitations of the model are discussed.

Graphene and carbon nanotubes are remarkable materials, notable for both their fascinating properties and their technological promise [1]. In both contexts, it is often necessary to calculate the phonons for problems where the use of *ab initio* methods is not feasible. For graphitic systems, this has usually been approached by approximating the force-constant matrix with terms coupling atoms up to some maximum distance [2, 3, 4, 5, 6, 7, 8]. This approach has many appealing features, but it has two important limitations. First, the terms in the force-constant matrix decay smoothly with distance between atoms [9], so in practice it is necessary to truncate the expansion long before it has converged. Second, this approach is generally restricted to describing phonons in the ideal crystal. It has required some ingenuity and inconvenience even to extend these models to nanotubes, based on an idealized curved-graphene structure [3, 4, 5, 6].

In order to treat phonons in large low-symmetry systems, such as rumbled graphene or bent nanotubes, one would like a model that explicitly gives the energy as a function of atomic positions, without reference to any underlying crystal structure. In principle one could use the general-purpose empirical interatomic potentials that are available for carbon, such as Ref. [10]. But phonon applications typically require higher accuracy than such general-purpose models can provide.

For diamond- and zinblende-structure semiconductors, the problem was largely solved by the use of “valence force” models. These models use a smaller number of more complex terms, which may be more or less physically motivated [11]. However, to date only one valence force model has been proposed for graphene [12, 13]; and it explicitly references the graphene lattice, hindering application to distorted structures [14].

Here we present a new valence force model for sp^2 -bonded carbon. The model explicitly gives energy as a function of atomic positions, without reference to any underlying crystal structure. The only restriction is that the local geometry be consistent with sp^2 bonding, i.e. three neighbors not too far from 120° degrees apart. Thus it can be directly applied not only to graphene, but to nanotubes and fullerenes, in relaxed or distorted configurations. We have tested the model for phonons in graphene

and carbon nanotubes. We first describe the model itself, and the fitting procedure. We then present and discuss the phonon spectrum which is obtained after fitting the model parameters to selected experimental and theoretical data. Finally we discuss the overall accuracy and limitations, along with some related issues such as anharmonicity.

We write the energy as

$$\begin{aligned}
 E = & \beta_{r1} r_0^{-2} \sum_{i,j \in i} (\delta r_{ij})^2 + \beta_c \sum_{i,j < k \in i} (\delta c_{i,jk})^2 \\
 & + \beta_v r_0^{-2} \sum_{i,j < k < l \in i} \left(\frac{3v_{ij} \cdot v_{ik} \times v_{il}}{r_{ij}r_{ik} + r_{ik}r_{il} + r_{il}r_{ij}} \right)^2 \\
 & + \beta_{r2} r_0^{-2} \sum_{i,j < k \in i} (\delta r_{ij}) (\delta r_{ik}) + \beta_p \sum_{i,j \in i} |\pi_i \times \pi_j|^2 \\
 & + \beta_{rc} r_0^{-1} \sum_{i,j \neq k < l \in i} (\delta r_{ij}) (\delta c_{i,kl}) \quad (1)
 \end{aligned}$$

where $v_{ij} = v_j - v_i$, v_i being the atomic position vector of atom i , and the bondlength is $r_{ij} = |v_{ij}|$. In the summations, $j \in i$ means j runs over three neighbors of atom i , $j < k \in i$ means j and k are both neighbors of i (ordered to avoid double counting), restriction $j < k < l$ leaves only one possibility for the three neighbors of i , while restriction $j \neq k < l$ gives three terms for each i .

The bond length in the ground state of graphene is $r_0 = 0.142$ nm; $\delta r_{ij} = r_{ij} - r_0$. We further define

$$\begin{aligned}
 \delta c_{i,jk} &= \frac{1}{2} + \frac{v_{ij} \cdot v_{ik}}{r_{ij}r_{ik}} \\
 \pi_i &= 3 \frac{v_{ij} \times v_{ik} + v_{ik} \times v_{il} + v_{il} \times v_{ij}}{r_{ij}r_{ik} + r_{ik}r_{il} + r_{il}r_{ij}} \quad (2)
 \end{aligned}$$

where j , k , and l are the three neighbors of i .

The first two terms in Eq. (1) represent the bond stretching stiffness β_{r1} and bending stiffness β_c , as in the Keating model [15]. However, the form here avoids the large and unphysical anharmonicities of the Keating model. The third term β_v provides stiffness against out-of-plane vibrations. The fourth term β_{rc} is motivated by bond-order potentials [10]. The fifth term β_p gives stiffness against misalignment of neighboring π orbital. The last term β_{rc} couples bond stretching and bond bending.

In fitting such a model, one typically chooses a set of data that it is desired to reproduce, and defines a weighted error which is to be minimized. As a straightforward test of the model and its ability to reproduce realistic phonon dispersions, we first try fitting to published LDA calculations [7, 16]. The result is shown in Fig. 1. [We follow the spectroscopic convention of reporting phonon energies in cm^{-1} , where 1 cm^{-1} means $hc/(1 \text{ cm}) \approx 0.124 \text{ meV}$.] The rms error is only 22.6 cm^{-1} , substantially less than the best previous fit to GGA dispersions using a valence force model with five parameters [13].

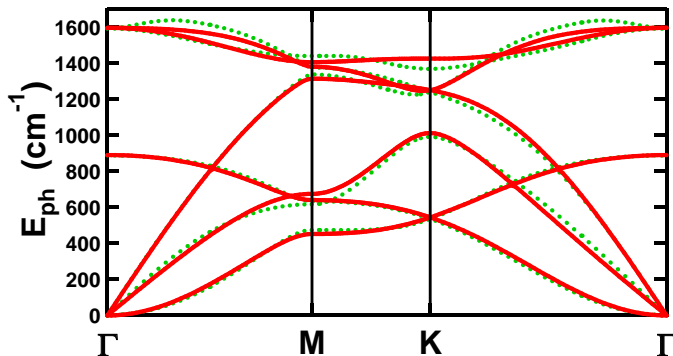


FIG. 1: Phonon band dispersions. Green dotted curves are LDA calculations [7]. Red solid curves are results of the model Eq. (1) fitted to these LDA calculations. The corresponding parameters are given in [16].

By giving more weight to one feature or another in the fitting, it is straightforward to improve the description of e.g. the acoustic branches at the cost of worsening the optical branches. However, regardless of how we weighted the data, we could not reproduce the dips in the highest phonon bands at Γ and K while keeping a reasonable overall dispersion. This issue was also mentioned in [13]. Electron-phonon interactions are known to affect phonon dispersions even in bulk semiconductors [9]; and such interactions are particularly important for the highest bands of graphene near Γ and K due to the Kohn anomaly [17]. Thus we cannot expect to describe these dips with short-range classical interactions. It would therefore seem logical to fit the bands away from Γ and K , and accept that the model gives energies that are too high for the top bands at those points. However, because the optical phonon energy at Γ is a widely used reference, we have chosen to fit this point accurately.

We find that the Poisson ratio calculated with our model fitted to the LDA calculations alone is $\nu = 0.4$, much less than the experimental value of $\nu = 0.17$. This suggests that elastic properties should be included in the fitting. Also, the experimental and theoretical data are not in perfect accord. We have therefore chosen to fit a mixture of published experimental phonon data, *ab initio* phonon calculations, and elastic constants. The resulting parameter values are listed in Table I, and the corre-

sponding phonon dispersion is shown as a solid curve in Figure 2. The corresponding elastic constants are given in Table II. (We equate in-plane elastic properties of graphene and graphite using the experimental layer spacing $c = 6.7 \text{ \AA}$ and volume per atom $V_0 = 3\sqrt{3}r_0^2c/8$.)

Overall we consider the agreement in Figure 2 and Table II to be quite good. The quality of the fit is a highly nonlinear function of the parameters, so there may be entirely different sets of parameters that give a similar or even better agreement with the same data.

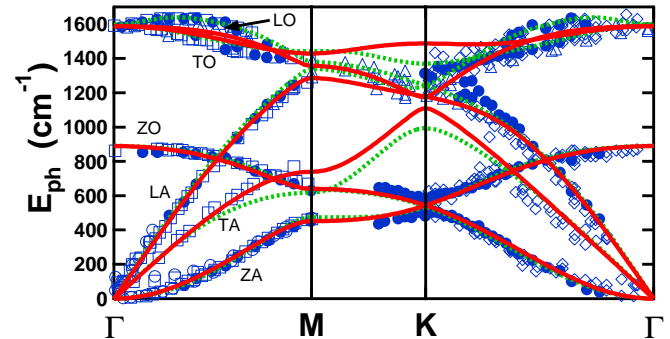


FIG. 2: Phonon band dispersion, comparing fitted model with experimental data and *ab initio* calculations. Red solid curve is our model, Eq. (1), with the parameters given in Table I. Green dotted curve is an LDA calculation [7]. Blue symbols are experimental data: electron energy loss spectroscopy (EELS) from Refs. [18], [19], and [20] (respectively squares, diamonds, and filled circles), neutron scattering from Ref. [21] (open circles), and x-ray scattering from Ref. [22] (triangles). Data for Refs. [18, 19, 20, 21, 22] are taken from Ref. [23].

TABLE I: Parameters of the model Eq. (1) used in Fig. 2, based on best fit to the experimental data and LDA calculations. Units are eV.

β_{r1}	β_c	β_v	β_{r2}	β_p	β_{rc}
18.52	4.087	1.313	4.004	0.008051	4.581

The longitudinal and transverse sound velocities ($v = d\omega/dq$ at $q = 0$) within our model are

$$M_C v_T^2 = \frac{81}{4} \frac{4\beta_{r1}\beta_c - 2\beta_{r2}\beta_c - \beta_{rc}^2}{12\beta_{r1} + 27\beta_c - 6\beta_{r2} - 18\beta_{rc}}$$

$$M_C v_L^2 = M_C v_T^2 + \frac{3}{2} (\beta_{r1} + \beta_{r2}) \quad (3)$$

where M_C is the mass of a carbon atom. The model velocities $v_{TA} \approx 13.3 \text{ km/s}$ and $v_{LA} \approx 21.2 \text{ km/s}$ are very close to the experimental values of $v_{TA} \approx 14 \text{ km/s}$ and $v_{LA} \approx 24 \text{ km/s}$ [18]. The elastic constants are related to the sound velocities: $V_0 C_{66} = M_C v_T^2$ and $V_0 C_{11} = M_C v_L^2$ [25].

It is often convenient to have analytic expressions for the phonon energies at symmetry points (e.g. for verifying a numerical implementation). From Eq. (1),

$$\omega^2 = (M_C r_0^2)^{-1} \sum_i \alpha_i \beta_i \quad (4)$$

where the index i runs over $(r1, c, v, r2, p, rc)$ and coefficients α_i are given in Table III.

Turning from graphene to carbon nanotubes, we calculate the radial breathing mode (RBM) for tubes of different diameter and chirality. This mode corresponds to a radial stretching or compression of the tube. The mode emerges from the lowest-energy acoustic phonon modes in graphene. The RBM acquires finite energy at zero wavevector due to the nanotube curvature, with a simple $\approx 1/d$ scaling of energy with diameter. As a result, RBM measurements are widely used to identify the diameters of single-walled carbon nanotubes [26].

For a given tube, we first relax the atomic positions and allow the lattice constant to adjust to minimize the energy. We then calculate the RBM energy. The results for all tubes in the diameter range from 0.5 to 4.0 nm are shown in Fig. 3. Simple scaling arguments based on continuum elasticity suggest that RBM energies should scale with diameter as $\hbar\omega_{RBM} = A/d$. Experimental data are typically fitted with the phenomenologically adapted form $\hbar\omega_{RBM} = A/d + B$. For tubes of $d=1$ nm, experimental phonon energies $A+B$ are reported in the range 226-248 cm^{-1} [27, 28, 29, 30, 31, 32, 33], while *ab-initio* calculations suggest $A+B=234$ or 226 cm^{-1} [27, 32]. The constant off-set was reported in the range from $B = -6$ cm^{-1} to $B = 27$ cm^{-1} . Recently, it was reported [33] that a non-zero offset B is caused by the interaction with a substrate, while for freely suspended nanotubes B should be zero.

Within our model, the RBM mode shows accurate A/d scaling independent of chirality, with $B \approx 0$ and $A \approx 225$ cm^{-1} (where d is in nm) as shown in Fig. 3. From the theory of elasticity, $A = 2\hbar v_L$, which gives $A \approx 225$ cm^{-1} for the parameters of Table I, in accord with the numerical result. The model is in good agreement with the most recent experimental [33] and theoretical [32] values of $A=227$ and $A+B=226$ cm^{-1} respectively.

In general, a valence force model will have some anharmonicity. Since we have not attempted to fit experimental or *ab initio* anharmonicities, any anharmonic-

TABLE II: Elastic constants from the experiment and the model (in GPa). Note a relation among elastic constants [14, 25] for hexagonal symmetry: $C_{66} = (C_{11} - C_{12})/2$, $\nu = C_{12}/C_{11}$.

	C_{11}	C_{12}	C_{66}	ν
experiment [24]	1060	180	440	0.17
model	1024	210	407	0.20

ities are likely to be unphysical. It is therefore desirable to minimize the anharmonicity in the model, and the form of Eq. (1) is designed with this in mind. One measure of anharmonicity is the Gruneisen parameter $\gamma = -(2\omega)^{-1}(d\omega/d\varepsilon)$, which represents the fractional shift in phonon frequency ω when the crystal is subjected to a strain ε in all directions. For the doubly degenerate E_{2g} phonon mode in graphene, our model gives $\gamma_{E_{2g}} \approx -0.2$. This is much smaller in magnitude than the experimental value of $\gamma_{E_{2g}} \approx 2.0$ [13, 34], confirming that our model is relatively harmonic in this respect.

For nanotubes, we have another form of anharmonicity, the phonon shifts due to bending of the graphene sheet. We have calculated the shifts in LO and TO phonons relative to graphene. The TO mode shift is less than 12 cm^{-1}/d^2 in our model (where d is in nm), and the LO mode and the LO-TO splitting are even less. Experimental shifts are four times larger in semiconducting nanotubes [35], confirming that our model successfully minimizes any unintended anharmonicities.

In conclusion, we have developed a valence force model applicable for sp^2 -carbon based structures. Our model gives a good fit of the graphene phonon dispersion and elastic constants, and describes well the RBM energy of nanotubes. The model also avoids the unphysical strong anharmonicities that occur in some valence force models. Most importantly, in contrast to other phonon models for sp^2 -bonded carbon, Eq. (1) makes no reference to an underlying lattice, so it can be directly applied to distorted geometries.

We gratefully acknowledge N. Marzari, O. Dubay, and D. Kresse for providing data for Figs. 2 and 1, and W. A. Harrison and A. Jorio for helpful discussions.

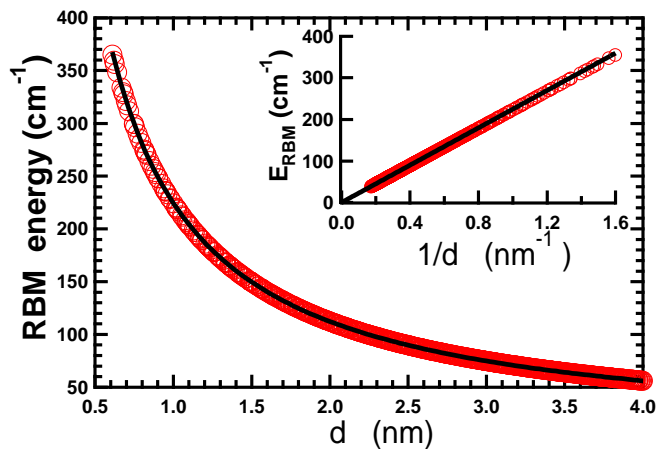


FIG. 3: Radial Breathing Mode (RBM) energy as a function of tube diameter (red open circles) along with the best fit $\hbar\omega_{RBM} = 224.6 \text{ cm}^{-1}/d$ (black solid curve). The inset shows the same results versus inverse diameter.

* Electronic address: vperebe@us.ibm.com

† Electronic address: tersoff@us.ibm.com

- [1] Ph. Avouris, Z. Chen, and V. Perebeinos, *Nature Nanotech.* **2**, 605 (2007).
- [2] R. Al-Jishi and G. Dresselhaus, *Phys. Rev. B* **26**, 4514 (1982).
- [3] R. A. Jishi, L. Venkataraman, M. S. Dresselhaus, and G. Dresselhaus, *Chem. Phys. Lett.* **209**, 77 (1993).
- [4] J.P. Lu, *Phys. Rev. Lett.* **79**, 1297 (1997).
- [5] R. Saito, T. Takeya, T. Kimura, G. Dresselhaus, and M. S. Dresselhaus, *Phys. Rev. B* **57**, 4145 (1998).
- [6] E. Dobardžić, I. Milošević, B. Nikolić, T. Vuković, and M. Damnjanović, *Phys. Rev. B* **68**, 045408 (2003).
- [7] O. Dubay and G. Kresse, *Phys. Rev. B* **67**, 035401 (2003).
- [8] M. Mohr, J. Maultzsch, E. Dobardzic, S. Reich, I. Milosevic, M. Damnjanovic, A. Bosak, M. Krisch, and C. Thomsen *Phys. Rev. B* **76**, 035439 (2007).
- [9] R. Sokel and W. A. Harrison, *Phys. Rev. Lett.* **36**, 61 (1976).
- [10] J. Tersoff, *Phys. Rev. Lett.* **56**, 632 (1986). [However actual applications should use later versions: J. Tersoff, *Phys. Rev. B* **37**, 6991 (1988); J. Tersoff, *Phys. Rev. Lett.* **61**, 2879 (1988).]
- [11] See E. O. Kane, *Phys. Rev. B* **31**, 7865 (1985); and references therein.
- [12] T. Aizawa, R. Souda, S. Otani, Y. Ishizawa, and C. Oshima, *Phys. Rev. B* **42**, 11469 (1990); **43**, 12060 (1991).
- [13] L. Wirtz and A. Rubio, *Solid State Comm.* **131** 141 (2004).
- [14] V. N. Popov, V. E. Van Doren, and M. Balkanski, *Phys. Rev. B* **59**, 8355 (1999); **61**, 3078 (2000).
- [15] P. N. Keating, *Phys. Rev.* **145**, 637 (1966).
- [16] The model parameters $\beta_{r1} = 19.39$, $\beta_c = 3.409$, $\beta_v = 1.318$, $\beta_{r2} = 8.364$, $\beta_p = 0.008078$, and $\beta_{rc} = 2.534$ (in eV) give the fit to LDA calculations shown in Fig.1, with the standard deviation of $\sigma = 22.6 \text{ cm}^{-1}$ and the maximum deviation of $|\hbar\omega_{model} - \hbar\omega_{LDA}| = 57 \text{ cm}^{-1}$. A similar fit quality can be achieved in fitting GGA phonon dispersions from Ref. [23]. However, we recommend using instead the parameters of Table I.
- [17] S. Piscanec, M. Lazzeri, F. Mauri, A. C. Ferrari, and J. Robertson, *Phys. Rev. Lett.* **93**, 185503 (2004).
- [18] C. Oshima, T. Aizawa, R. Souda, Y. Ishizawa, and Y. Sumiyoshi, *Solid State Commun.* **65**, 1601 (1988).
- [19] S. Siebentritt, R. Pues, K-H. Rieder, and A. M. Shikin *Phys. Rev. B* **55**, 7927 (1997).
- [20] H. Yanagisawa, T. Tanaka, Y. Ishida, M. Matsue, E. Rokuta, S. Otani, and C. Oshima, *Surf. Interface Anal.* **37**, 133 (2005).
- [21] R. Nicklow, N. Wakabayashi, and H. G. Smith, *Phys. Rev. B* **5**, 4951 (1972).
- [22] J. Maultzsch, S. Reich, C. Thomsen, H. Requardt, and P. Ordejon, *Phys. Rev. Lett.* **92**, 075501 (2004).
- [23] N. Mounet and N. Marzari, *Phys. Rev. B* **71**, 205214 (2005).
- [24] O.L. Blakslee, D.G. Proctor, E.J. Seldin, G.B. Spence, and T. Weng, *J. Appl. Phys.* **41**, 3373 (1970).
- [25] L. D. Landau and E. M. Lifshitz, *Theory of Elasticity* (Pergamon, London, 1959).
- [26] A. Jorio, M. S. Dresselhaus, and G. Dresselhaus, *Carbon Nanotubes: Advanced Topics in Synthesis, Properties, and Applications*, Topics in Applied Physics Vol. 111 (Springer, Berlin, 2008).
- [27] J. Kuřti, G. Kresse, and H. Kuzmany, *Phys. Rev. B* **58**, R8869 (1998).
- [28] A. Jorio, R. Saito, J. H. Hafner, C. M. Lieber, M. Hunter, T. McClure, G. Dresselhaus, and M. S. Dresselhaus, *Phys. Rev. Lett.* **86**, 1118 (2001).
- [29] S. M. Bachilo, M. S. Strano, C. Kittrell, R. H. Hauge, R. E. Smalley, and R. B. Weisman, *Science* **298**, 2361 (2002).
- [30] H. Telg, J. Maultzsch, S. Reich, F. Hennrich, and C. Thomsen, *Phys. Rev. Lett.* **93**, 177401 (2004).
- [31] J. C. Meyer, M. Paillet, T. Michel, A. Moreac, A. Neumann, G. S. Duesberg, S. Roth, and J.-L. Sauvajol, *Phys. Rev. Lett.* **95**, 217401 (2005).
- [32] M. Machon, S. Reich, H. Telg, J. Maultzsch, P. Ordejon, and C. Thomsen, *Phys. Rev. B* **71**, 035416 (2005).
- [33] P. T. Araujo, I. O. Maciel, P. B. C. Pesce, M. A. Pimenta, S. K. Doorn, H. Qian, A. Hartschuh, M. Steiner, L. Grigorian, K. Hata, and A. Jorio, *Phys. Rev. B* **77**, 241403(R) (2008).
- [34] T. M. G. Mohiuddin, A. Lombardo, R. R. Nair, A. Bonetti, G. Savini, R. Jalil, N. Bonini, D.M. Basko, C. Galiotis, N. Marzari, K. S. Novoselov, A. K. Geim, A. C. Ferrari, arXiv:0812.1538.
- [35] A. Jorio, A. G. Souza Filho, G. Dresselhaus, M. S. Dresselhaus, A. K. Swan, M. S. Unlu, B. B. Goldberg, M. A. Pimenta, J. H. Hafner, C. M. Lieber, and R. Saito, *Phys. Rev. B* **65**, 155412 (2002).

TABLE III: Exact coefficients α_i for the analytical expressions Eq. (4) of phonon energies at high symmetry k points.

k point	mode	$\hbar\omega \text{ cm}^{-1}$	α_{r1}	α_c	α_v	α_{r2}	α_p	α_{rc}
Γ	ZO	889	0	0	54	0	0	0
	LO/TO	1588	12	27	0	-6	0	-18
M	ZA	452	0	0	6	0	1296	0
	ZO	640	0	0	24	0	648	0
	TA	740	0	12	0	0	0	0
	LA	1286	8	0	0	0	0	0
	LO	1357	4	27	0	2	0	-6
	TO	1429	12	3	0	-6	0	-6
K	ZO/ZA	544	0	0	13.5	0	1093.5	0
	TA	1110	0	27	0	0	0	0
	LO/LA	1177	6	6.75	0	1.5	0	-4.5
	TO	1487	12	0	0	-6	0	0